Effects of the polyfluoroalkyl side-chain on the properties of

1-methyl-3-polyfluoroalkylimidazolium fluorohydrogenate ionic liquids

Ryosuke Taniki, Naoki Kenmochi, Kazuhiko Matsumoto*, Rika Hagiwara

Graduate School of Energy Science, Kyoto University, Sakyo-ku, Kyoto 606-8501, Japan,

*E-mail: k-matsumoto@energy.kyoto-u.ac.jp

Tel: +81-75-753-5822

Fax: +81-75-753-5906

Abstract

A series of 1-methyl-3-polyfluoroalkylimidazolium fluorohydrogenate salts ($C_{3F3}MIm(FH)_{1.7}F$, $C_{4F5}MIm(FH)_{1.7}F$, $C_{6F9}MIm(FH)_{1.8}F$, $C_{8F13}MIm(FH)_{2.0}F$, and $C_{10F17}MIm(FH)_{2.0}F$; the subscript numbers denote the number of carbon and fluorine atoms in the side-chain, respectively, with which the two carbon atoms from the root of the side-chain are not fluorinated) were synthesized and their physicochemical properties, including decomposition temperature, phase transition temperature, density, viscosity, ionic conductivity, and electrochemical stability, were measured. The three salts with relatively short side-chain have melting points below room temperature; $C_{3F3}MIm(FH)_{1.7}F$ (T_m: 274 K), $C_{4F5}MIm(FH)_{1.7}F$ (T_g: 186 K), and $C_{6F9}MIm(FH)_{1.8}F$ (T_m: 276 K). The other salts, $C_{8F13}MIm(FH)_{2.0}F$ and $C_{10F17}MIm(FH)_{2.0}F$, are in the crystal phase at room temperature. The obtained salts are miscible with water and hydrophobic fluorohydrogenate ionic liquids were not obtained in the present series. Introduction of fluorine atoms results in the increase in the density and viscosity, decrease in the ionic conductivity, and decrease in electrochemical stability against reduction. The liquid crystal phase was observed for $C_{8F13}MIm(FH)_{2.0}F$ and $C_{10F17}MIm(FH)_{2.0}F$ according to polarized optical microscopy and X-ray diffraction analysis.

1. Introduction

Ionic liquids (ILs) are liquid composed of only organic and/or inorganic ions without containing neutral species. In particular, ILs with melting points below room temperature are called room temperature ionic liquids (RTILs) [1–4]. The report about the first air-stable IL, 1-ethyl-3-methylimidazolium tetrafluoroborate (EMImBF$_4$), triggered many researchers to find new ILs with a wide variety of properties by the combination of various cations and anions [5]. The unique properties often found for ILs are extremely low vapor pressure, non-flammability, good thermal and electrochemical stability, wide liquid phase temperature range, high polarity, and catalytic properties. The ILs can be utilized as stable electrolytes in batteries, capacitors, fuel cells, dye-sensitized solar cells, and electrolytic bath, and as clean solvent and catalyst for various organic reactions, enzyme reactions, phase separations, and extractions [6–10].

Fluoroanions, such as BF_4^-, PF_6^-, $CF_3SO_3^-$, $(CF_3SO_2)_2N^-$, and $(FSO_2)_2N^-$, are frequently used as counteranions in ILs [4]. Fluorohydrogenate anion $((FH)_nF^-)$ is one of them and gives highly conductive and low viscous ILs called fluorohydrogenate ILs (FHILs) in combination of various cations (1-alkyl-3-methylimidazolium, *N*-alkylpyridinium, *N*-alkyl-*N*-methylpyrrolidinium, *N*-alkyl-*N*-methylpiperidinium, tetraalkylphosphonium, and trialkylsulfonium) [11–16]. For example, 1-ethyl-3-methylimidazolium fluorohydrogenate (EMIm(FH)$_{2.3}$F) is nonvolatile, nonflammable, stable in the air, and inert against borosilicate glass in spite of the anions containing a HF unit, and possesses a high ionic conductivity of 100 mS cm^{-1} and low viscosity of 4.9 cP at 298 K, as well as a low melting temperature of 208 K [11,12]. Fluorohydrogenate anions are oligomeric complex ions, where several HF units are bound as ligands to the central fluorine atom. The HF unit is rapidly exchanging between $(FH)_2F^-$ and $(FH)_3F^-$ according to NMR study and behaves like a solvent molecule with a certain dipole moment to weaken the cation–anion interaction [17,18]. Hence, the effective radii of the anionic species actually migrating in FHILs become small by the exchange of ligand HF between the anions. The low viscosity and high ionic

conductivity of FHILs lead to the applications as electrolytes in electrochemical capacitors, fuel cells, and dye-sensitized solar cell [19–21].

Ionic liquids based on polyfluoroalkylated cations have been studied as hydrophobic ILs with some interesting properties; inertness to organic solvents and oxidizing agents, resistance to corrosive acids and bases, and resistance to extremes of temperature and pressure [22–27]. These ILs were mainly applied as reaction solvents for organic reactions and separations as well as catalysis due to their unique properties [22], whereas there are little reports about the usage as electrolytes for electrochemical devices. In this study, fluorohydrogenate salts based on polyfluoroalkylated imidazolium cations are synthesized and characterized, and the effects of the polyfluoroalkyl side-chain on the physicochemical properties of fluorohydrogenate salts are discussed.

2. Results and discussion

2.1 Synthesis and general properties

The numbers of fluorine atoms in the side-chain of 1-methyl-3-polyfluoroalkylimidazolium cations ($C_{(x+2)F(2x+1)}MIm^+$, x is the number of carbon atoms with fluorine atoms) in this study are 3 ($C_{3F3}MIm^+$: 1-methyl-3-(3,3,3-trifluoropropyl)imidazolium), 5 ($C_{4F5}MIm^+$: 1-methyl-3-(3,3,4,4,4-pentafluorobutyl)imidazolium), 9 ($C_{6F9}MIm^+$: 1-methyl-3-(3,3,4,4,5,5,6,6,6-nonafluorohexyl)imidazolium), 13 ($C_{8F13}MIm^+$: 1-methyl-3-(3,3,4,4,5,5,6,6,7,7,8,8,8-tridecafluorooctyl)imidazolium), and 17 ($C_{10F17}MIm^+$: 1-methyl-3-(3,3,4,4,5,5,6,6,7,7,8,8,9,9,10,10,10-heptadecafluorodecyl)imidazolium), with which the two carbon atoms from the root of the side-chain are not fluorinated as shown in Fig. 1. All the $C_{(x+2)F(2x+1)}MIm(FH)_nF$ salts were prepared by reaction of the corresponding iodide and excess anhydrous HF. In order to compare the effects of fluorine atoms, 1-methyl-3-propylimidazolium fluorohydrogenate ($C_3MIm(FH)_{1.7}F$) was synthesized and characterized, where $C_{3F3}MIm(FH)_{1.7}F$

and $C_3MIm(FH)_{1.7}F$ have the same number of carbon atoms and there is only the difference between terminal methyl group and trifluoromethyl group in the side-chain. At room temperature, $C_{3F3}MIm(FH)_{1.7}F$, $C_{4F5}MIm(FH)_{1.7}F$, and $C_{6F9}MIm(FH)_{1.8}F$ are liquid, while $C_{8F13}MIm(FH)_{2.0}F$ and $C_{10F17}MIm(FH)_{2.0}F$ are powdery solid. The $(FH)_nF^-$ anions were identified by infrared (IR) spectroscopy (Fig. S1). Two solid salts have the vacuum-stable HF content of 2.0 ($C_{8F13}MIm(FH)_{2.0}F$ and $C_{10F17}MIm(FH)_{2.0}F$), suggesting the formation of the one to one crystal phase of the cations and $(FH)_2F^-$, while the other three RTILs have the lower HF content ($C_{3F3}MIm(FH)_{1.7}F$, $C_{4F5}MIm(FH)_{1.7}F$, and $C_{6F9}MIm(FH)_{1.8}F$). Previous reports show that the vacuum-stable HF content in FHILs based on imidazolium, pyridinium, pyrrolidinium, and piperidinium cations with short side-chains is 2.3 and those with long side-chains are below 2.3 [13,14,28,29]. This trend was not adapted to the present FHILs based on polyfluoroalkylated cations. Long side-chain or polyfluoroalkylated side-chain give strong van der Waals interactions between the side-chains, which may affect the cation-anion interactions and lower the vacuum-stable HF content. Fluorine containing materials often enhance hydrophobicity due to their low polarity. In the present study, all the $C_{(x+2)F(2x+1)}MIm(FH)_nF$ salts give a biphasic system at first when contacted with water. However, they slowly dissolved into water and form a single phase after a while although the whole fluorine weight in formula weight in cation is over 50%. Fluorohydrogenate anions are highly polar and form strong interactions with water, resulting in the strong hydrophilicity that overcomes the hydrophobicity of $C_{(x+2)F(2x+1)}MIm^+$. The massive introduction of fluorine atom together with extension of the side-chain in this study was not sufficient to give hydrophobicity of FHILs. On the other hand, the mixture of water and $C_{(x+2)F(2x+1)}MIm(FH)_nF$ made bubbles when vigorously agitated because the cations with separated polar and non-polar regions show an interfacial activity.

2.2 Thermal properties

Thermogravimetric (TG) curves of $C_{(x+2)F(2x+1)}MIm(FH)_nF$ and $C_3MIm(FH)_{1.7}F$ are shown in Fig. 2. Thermal decomposition temperatures based on the onset of large weight loss for $C_{(x+2)F(2x+1)}MIm(FH)_nF$ and $C_3MIm(FH)_{1.7}F$ are around 460 and 530 K, respectively. Gradual weight loss below the decomposition temperature is caused by HF dissociation from $(FH)_nF^-$. The introduction of polyfluoroalkyl side-chain in the cation lowers the thermal stability of the FHIL. Pyrolysis of imidazolium halides occurs by an S_N2 reaction, where the halide ion attacks α-carbon and alkylimidazole leaves [30]. Steric effects of side-chain in the imidazolium cation are weaker for short side-chain than long side-chain, resulting in the preferential break of C–N bond between nitrogen in imidazolium and α-carbon in short side-chain, and resulting in the formation of imidazole with the long side-chain as a leaving group [30]. In addition, the S_N2 reaction rate for pyrolysis is high in the case of the leaving group with low Lewis basicity. In the present cases, the main leaving group in pyrolysis of $C_{3F3}MIm(FH)_{1.7}F$ and $C_3MIm(FH)_{1.7}F$ is thought to be 1-(3,3,3-trifluoropropyl)imidazole and 1-propylimidazole, respectively. Because the polyfluoroalkyl side-chain withdraws the electron from the aromatic ring through ethylene group and lowers the Lewis basicity of 1-(3,3,3-trifluoropropyl)imidazole compared to that of 1-propylimidazole, thermal decomposition of $C_{3F3}MIm(FH)_{1.7}F$ would be accelerated compared to that of $C_3MIm(FH)_{1.7}F$. In the cases of the cations with longer polyfluorinated side-chains, the clear difference of decomposition behavior was not observed because fluorine atoms distant from the aromatic ring do not effectively withdraw the electrons from the ring.

Differential scanning calorimetric (DSC) curves of $C_{(x+2)F(2x+1)}MIm(FH)_nF$ and $C_3MIm(FH)_{1.7}F$ are shown in Fig. 3. Two RTILs, $C_{3F3}MIm(FH)_{1.7}F$ and $C_{6F9}MIm(FH)_{1.8}F$, have large endothermic peaks corresponding to melting. The $C_{4F5}MIm(FH)_{1.7}F$ salt exhibits only a glass transition. In the DSC curve of $C_{8F13}MIm(FH)_{2.0}F$, large endothermic and small endothermic peaks are observed at 326 and 382 K, respectively. As described below, the former peak shows a phase transition from the crystal phase to liquid crystal phase (melting) and the latter peak shows a phase

transition from liquid crystal phase to isotropic liquid phase (clearing). In the DSC curve of $C_{10F17}MIm(FH)_{2.0}F$, a large endothermic peak (melting) is observed at 349 K, whereas the peak corresponding to clearing is not observed because the clearing temperature is higher than its decomposition temperature.

2.3 Physicochemical properties

Physicochemical properties of $C_{(x+2)F(2x+1)}MIm(FH)_nF$ and $C_3MIm(FH)_{1.7}F$ are summarized in Table 1. Introduction of fluorine atoms increases density as observed in the comparison between $C_{3F3}MIm(FH)_{1.7}F$ (1.35 g cm^{-3}) and $C_3MIm(FH)_{1.7}F$ (1.12 g cm^{-3}). The large density of $C_{3F3}MIm(FH)_{1.7}F$ originates from the large difference in atomic weight and the small difference in size between fluorine and hydrogen atoms [31–33], where the difference of the formula weight is large (232 for $C_{3F3}MIm(FH)_{1.7}F$ and 178 for $C_3MIm(FH)_{1.7}F$, respectively) and the difference of molar volume, calculated by FW/ρ, is small (172 cm^3 mol^{-1} for $C_{3F3}MIm(FH)_{1.7}F$ and 159 cm^3 mol^{-1} for $C_3MIm(FH)_{1.7}F$, respectively). The increasing number of fluorine atoms increases the ratio of the whole fluorine weight to the formula weight of the cation, 31.8% for $C_{3F3}MIm^+$, 41.5% for $C_{4F5}MIm^+$, and 52.0% for $C_{6F9}MIm^+$, respectively, which reflects the increase in density.

The $C_{3F3}MIm(FH)_{1.7}F$ (28 cP at 298 K) salt exhibits a higher viscosity than $C_3MIm(FH)_{1.7}F$ (13 cP at 298 K). Fluorous interaction between adjacent cations is a possible reason for this phenomenon [34]. An electrostatic interaction between the negatively charged fluorine atoms in the polyfluoroalkyl group and the positively charged nitrogen and hydrogen atoms in the imidazolium ring might enhance the intermolecular interaction, resulting in the higher viscosity. Extension of polyfluoroalkyl side-chain leads to higher viscosities (87 cP for $C_{4F5}MIm(FH)_{1.7}F$ and 169 cP for $C_{6F9}MIm(FH)_{1.8}F$) because the fluorous interaction between polyfluoroalkyl side-chains increases [34]. Figure 4 shows Arrhenius plots of viscosity and ionic conductivity for the present RTILs and Table 2 lists activation energies obtained from these plots. The ionic conductivity decreases with

increase in the viscosity for any salts. Both activation energies increase with introducing a larger number of fluorine atoms. A similar tendency and relatively small discrepancy between the activation energies of viscosity and ionic conductivity suggest that high ionic conductivity is explained by low viscosity without introducing some special conduction mechanism such as ion hopping.

Linear sweep voltammograms of $C_{3F3}MIm(FH)_{1.7}F$ and $C_3MIm(FH)_{1.7}F$ are shown in Fig. 5. The electrochemical stability of $C_3MIm(FH)_{1.7}F$ is similar to $C_3MIm(FH)_{2.3}F$ in spite of the different HF content. The anodic limit of $C_3MIm(FH)_{1.7}F$ is considered to be oxidation of imidazolium cations, including fluorination by fluorohydrogenate anions, about 1 V vs. Fc^+/Fc [28]. For $C_{3F3}MIm(FH)_{1.7}F$ in Fig. 5, the first oxidation at about 1 V vs. Fc^+/Fc is similar to the case for $C_3MIm(FH)_{1.7}F$ and an improvement of electrochemical stability to oxidation by introducing fluorine atoms was not observed. The smaller current of the first oxidation and the following smaller current below the second oxidation at around 2 V vs. Fc^+/Fc indicates that the oxidation product of $C_{3F3}MIm(FH)_{1.7}F$ restricts further oxidation more than that of $C_3MIm(FH)_{1.7}F$. The higher onset potential of the second oxidation for $C_{3F3}MIm(FH)_{1.7}F$ shows that $C_{3F3}MIm(FH)_{1.7}F$ has a higher stability to further oxidation than $C_3MIm(FH)_{1.7}F$. On the other hand, electrochemical stability of $C_{3F3}MIm(FH)_{1.7}F$ against reduction is poorer than that of $C_3MIm(FH)_{1.7}F$ because the high electrophilicity of polyfluoroalkyl side-chains raise the acidity of the imidazolium ring.

2.4 Liquid crystalline behavior

Figure 6 shows polarized optical microscopic (POM) textures of $C_{8F13}MIm(FH)_{2.0}F$ and $C_{10F17}MIm(FH)_{2.0}F$ at 373 K. The former was obtained by cooling the isotropic liquid to obtain liquid crystal, whereas the latter was obtained by heating the crystal because $C_{10F17}MIm(FH)_{2.0}F$ decomposes without clearing. A fan-like texture spontaneously formed in both the cases. The POM image suggests that the liquid crystal has a smectic structure as observed in other imidazolium ionic

liquid crystals [29].

Figures 7 and S2 show the X-ray diffraction (XRD) patterns of the crystal and liquid crystal phases for $C_{8F13}MIm(FH)_{2.0}F$ in the low-angle and wide-angle ranges, respectively. In the crystal phase, the diffraction peaks are observed over a wide range of angle, whereas those in the liquid crystal are observed only in the low-angle region. The sharp peaks observed in the low-angle region for both the crystal (e.g., 2.75° at 293 K) and liquid crystal (e.g., 3.07° at 333 K) phases indicate formation of layered structures. The shaper peaks in the crystal phase than those in the liquid crystal phase result from the more highly ordered structure of the cations in the crystal phases. Similar phenomenon was observed in 1-dodecyl-3-methylimidazolium fluorohydrogenate ($C_{12}MIm(FH)_{2.0}F$) salts [29]. The two more peaks are observed in the lower angle region than that for the sharp peak found for the crystal phase and may result from the in-plane ordering the layer. The weak peak around 6.3° observed in the liquid crystal phase corresponds to the 002 diffraction of the smectic phase. The effect of introducing fluorine atoms on the formation of the liquid crystal is confirmed by comparing $C_{8F13}MIm(FH)_{2.0}F$ and 1-methyl-3-octylimidazolium fluorohydrogenate ($C_8MIm(FH)_{2.0}F$), between which the difference is the existence of fluorine atoms [29]. The $C_8MIm(FH)_{2.0}F$ salts does not form the liquid crystal phase, whereas $C_{8F13}MIm(FH)_{2.0}F$ does due to the strong fluorous interaction between two side-chains. The POM image of $C_{10F17}MIm(FH)_{2.0}F$ indicates the phase found above 349 K is the liquid crystal phase, whereas the confirmation of liquid crystal by XRD at such high temperatures was technically difficult.

The layer spacings (*d*) for crystals and liquid crystals of $C_{8F13}MIm(FH)_{2.0}F$ are shown in Fig. 8. Figure 9 shows a schematic illustration of the crystal–liquid crystal phase transition of $C_{8F13}MIm(FH)_{2.0}F$. The layer spacing of the liquid crystal in $C_{8F13}MIm(FH)_{2.0}F$ is smaller than that of the crystal, which contradicts the general trend for previously known analogues with non-fluoroalkyl side-chains [29,35,36]. The size of $C_{8F13}MIm^+$ along the long axis (from the carbon in the methyl group to the fluorine at the end of the polyfluoroalkyl group) is roughly estimated to

be 15 Å according to previous crystallographic works, assuming the polyfluoroalkyl side-chain adopts all-trans conformation [37,38]. The layer spacing in the $C_{8F13}MIm(FH)_{2.0}F$ crystal (32.1 Å at 293 K) is much larger than that of $C_{12}MIm(FH)_{2.0}F$ crystal even with a longer side-chain (26.6 Å for at 283 K) [29], and nearly twice larger than the $C_{8F13}MIm^+$ size along the long axis, which suggests that interdigitation does not occur in the bilayer structure of the crystal and that the layer spacing can become much smaller by deeply interdigitating the polyfluoroalkyl side-chains each other when the polyfluoroalkyl side-chains become more fluid by melting.

3. Conclusions

New fluorohydrogenate salts based on $C_{(x+2)F(2x+1)}MIm(FH)_nF$ were synthesized and characterized. These salts are miscible with water. Three RTILs were obtained; $C_{3F3}MIm(FH)_{1.7}F$ (T_m: 274 K) $C_{4F5}MIm(FH)_{1.7}F$ (T_g: 186 K), and $C_{6F9}MIm(FH)_{1.8}F$ (T_m: 276 K), whereas the other salts, $C_{8F13}MIm(FH)_{2.0}F$ and $C_{10F17}MIm(FH)_{2.0}F$, were in the crystal phase at room temperature. The introduction of fluorine atoms resulted in the increase in the density and viscosity, decrease in the ionic conductivity, and lower electrochemical stability to reduction. The liquid crystal phase was observed in $C_{8F13}MIm(FH)_{2.0}F$ and $C_{10F17}MIm(FH)_{2.0}F$. Introducing fluorine atoms promotes the formation of the liquid crystal phase, whereas the interdigitation of polyfluoroalkyl side-chains does not occur in the crystal phase.

4. Experimental

4.1 General experimental procedure

Volatile materials were handled using a vacuum line constructed of SUS316 stainless–steel and tetrafluoroethylene–perfluroalkylvinylether copolymer (PFA). Nonvolatile materials were handled in a glove box under a dry Ar atmosphere. According to the previous report [23], the starting iodides $C_{(x+2)F(2x+1)}MImI$ were prepared by reactions of 1-methylimidazole (Aldrich, 99%)

and nearly equimolar quantities of the corresponding polyfluoroalkyl iodides, 3,3,3-trifluoropropyl iodide (Wako Pure Chemical Industries, 97%), 3,3,4,4,4-pentafluorobutyl iodide (Fluka, >99%), 3,3,4,4,5,5,6,6,6-nonafluorohexyl iodide (Tokyo Chemical Industry Co., 99.5%), 3,3,4,4,5,5,6,6,7,7,8,8,8-tridecafluorooctyl iodide (Aldrich, 96%), and 3,3,4,4,5,5,6,6,7,7,8,8,9,9,10,10,10-heptadecafluorodecyl iodide (Aldrich, 96%), at 353 K for two days. Purification of $C_{3F3}MImI$ was performed by washing with ethyl acetate (Wako Pure Chemical Industries, water content < 50 ppm) several times and recrystallization from the acetonitrile (Wako Pure Chemical Industries, water content < 50 ppm) solution by adding ethyl acetate. Purification of $C_{4F5}MImI$, $C_{6F9}MImI$, and $C_{8F13}MImI$ was performed by washing with ethyl acetate several times, chromatography using the activated alumina column with acetone (Wako Pure Chemical Industries, 99.5%), and recrystallization from the acetone solution by adding diethyl ether (Wako Pure Chemical Industries, 99.5%). Purification of $C_{10F17}MImI$ was performed by washing with ethyl acetate several times, chromatography using the activated alumina column with acetone, and recrystallization from the acetone solution by adding ethyl acetate. Finally the purified iodides were dried under vacuum at 353 K. See supporting information for the results of elemental analysis of $C_{(x+2)F(2x+1)}MImI$. Anhydrous HF (Daikin Industries) was dried over K_2NiF_6 prior to use.

4.2 Synthesis of $C_{(x+2)F(2x+1)}MIm(FH)_nF$ and $C_3MIm(FH)_{1.7}F$

The starting iodides, $C_{(x+2)F(2x+1)}MImI$, were weighed in a PFA reactor under a dry Ar atmosphere and a large excess of anhydrous HF was distilled on that at 77 K through the vacuum line. The mixture reacted on warming up to room temperature and the volatile gases were roughly eliminated by evacuation through a chemical and cold trap using a rotary pump. Elimination of the volatile gases and addition of fresh HF were repeated for effective elimination of iodide in the form of hydrogen iodide from the salt. The HF content of fluorohydrogenate salts were determined by titration using aq. 0.1029 M NaOH and weight change before and after the reaction with HF.

$C_3MIm(FH)_{1.7}F$; IR (AgCl): $\nu = 2340$ (m), 1985 (m), 1807 (s), 1045 (w) cm^{-1}, $C_{3F3}MIm(FH)_{1.7}F$; IR (AgCl): $\nu = 2337$ (m), 1983 (m), 1807 (s), 1021 (w) cm^{-1}, $C_{4F5}MIm(FH)_{1.7}F$; IR (AgCl): $\nu = 2350$ (m), 1981 (m), 1811 (s), 1022 (w) cm^{-1}, $C_{6F9}MIm(FH)_{1.8}F$; IR (AgCl): $\nu = 2350$ (m), 1979 (m), 1811 (s), 1036 (w) cm^{-1}, $C_{8F13}MIm(FH)_{2.0}F$; IR (AgCl): $\nu = 2340$ (m), 1977 (m), 1813 (s), 1042 (w) cm^{-1}, and $C_{10F17}MIm(FH)_{2.0}F$; IR (AgCl): $\nu = 2350$ (m), 1981 (m), 1815 (s), 1042 (w) cm^{-1} [$(FH)_2F^-$, see Fig. S1 for their IR spectra].

4.3 Analytical methods

Infrared spectra of solid and liquid samples were obtained by FTS-165 (BIO-RAD Laboratories). The samples were sandwiched between a pair of AgCl crystal windows in an airtight cell made of stainless steel. The TG analysis was performed under a dry Ar gas flow using Shimadzu DTG-60H at the scanning rate of 10 K min^{-1}. The sample was placed in a Ni open cell. The DSC analyses were performed under a dry Ar gas flow using Shimadzu DSC-60 at the scanning rate of 5 K min^{-1}. The sample was placed in a sealed cell made of stainless steel. Viscosity was measured by a cone and plate rheometer, LVDV-II+PRO (Brookfield Engineering Laboratories, Inc.), using the spindle of CPE-40. The samples were enclosed in the apparatus under a dry argon atmosphere in a glove bag. Density was measured under a dry argon atmosphere at room temperature by weighing the samples in a hand-made PFA vessel of which the volume was calibrated by distilled water and ethanol. Ionic conductivity was measured by an AC impedance technique using a calibrated cell with a pair of platinum disk electrodes with the aid of VSP (Bio-Logic) electrochemical measurement system. The ionic conductivity data were measured after the sample was held at the target temperature for at least 1 hr. The steadiness of the ionic conductivity value was confirmed by plotting it against time during this period. Electrochemical stability was investigated by linear sweep voltammetry under a dry Ar atmosphere with the aid of VSP electrochemical measurement system. Vitreous carbon electrodes were used as the working

and counter electrodes. A silver wire immersed in $EMImBF_4$ containing 0.05 M $AgBF_4$ was used for the reference electrode which was partitioned from the electrolyte with a porous PTFE filter (POREX, 7 μm pore). Polarized optical microscopy was carried out using a VHX digital microscope (Keyence) under cross-polarized light at $\times100$ magnification. The sample was placed in a transparent cell made of sapphire and covered with a piece of glass substrate. The temperature was controlled by TS1500 hot stage unit (Japan High Tech). X-ray diffraction was performed using a Rigaku Ultima IV diffractometer (Cu Kα, λ = 1.542 Å). The output power was set as 40 kV–40 mA. The data were recorded in the 2θ range of 2–30° (scanning rate of 1° per minute) with a step of 0.01°.

Appendix A. Supplementary data

Supplementary data associated with this article can be found, in the online version, at doi:xxxxxx.

Table 1 Physicochemical properties of the present fluorohydrogenate salts.

	Fw	T_m / K	T_c / K	ρ / g cm^{-3}	η / cP	σ / mS cm^{-1}
C$_3$MIm(FH)$_{1.7}$F	178	152 (T_g)	n.o.	1.12	13	31
C$_{3F3}$MIm(FH)$_{1.7}$F	232	274	n.o.	1.35	28	13
C$_{4F5}$MIm(FH)$_{1.7}$F	282	186 (T_g)	n.o.	1.43	87	5.6
C$_{6F9}$MIm(FH)$_{1.8}$F	384	276	n.o.	1.53	169	2.4
C$_{8F13}$MIm(FH)$_{2.0}$F	488	326	382	–	–	–
C$_{10F17}$MIm(FH)$_{2.0}$F	588	349	dec.	–	–	–

Fw: formula weight, T_m: melting point, T_g: glass transition temperature, T_c: clearing temperature, ρ: density at 298 K, η: viscosity at 298 K, σ: conductivity at 298 K, n.o.: not observed..

Table 2 Activation energies calculated from the Arrhenius plots of viscosities and ionic conductivities for the present RTILs.

	Activation energy of viscosity / kJ mol^{-1}	Activation energy of conductivity / kJ mol^{-1}
$C_3MIm(FH)_{1.7}F$	20.0	17.4
$C_{3F3}MIm(FH)_{1.7}F$	27.4	21.2
$C_{4F5}MIm(FH)_{1.7}F$	32.9	28.2
$C_{6F9}MIm(FH)_{1.8}F$	38.8	30.1
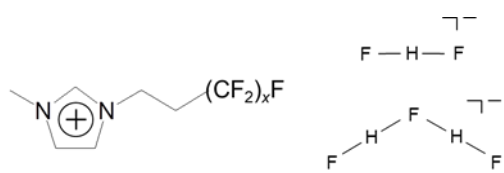
Fig. 1 Structures of $C_{(x+2)F(2x+1)}MIm^+$ (x = 1,2,4,6,8), FHF⁻, and (FH)₂F⁻.
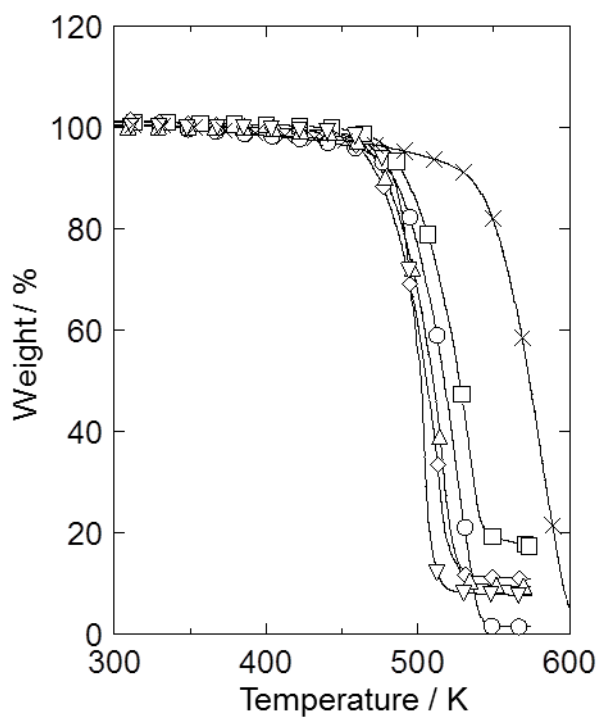
Fig. 2 Thermogravimetric curves of $C_3MIm(FH)_{1.7}F$ (×), $C_{3F3}MIm(FH)_{1.7}F$ (○), $C_{4F5}MIm(FH)_{1.7}F$ (□), $C_{6F9}MIm(FH)_{1.8}F$ (◇), $C_{8F13}MIm(FH)_{2.0}F$ (△), and $C_{10F17}MIm(FH)_{2.0}F$ (▽).
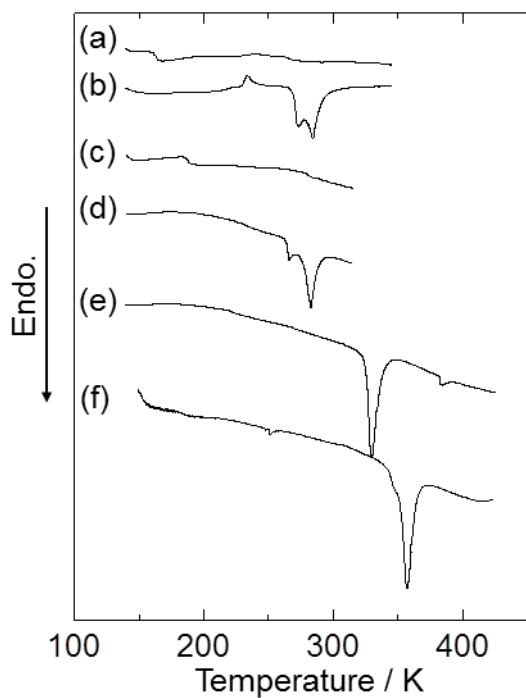
Fig. 3 Differential scanning calorimetric curves of (a) $C_3MIm(FH)_{1.7}F$, (b) $C_{3F3}MIm(FH)_{1.7}F$, (c) $C_{4F5}MIm(FH)_{1.7}F$, (d) $C_{6F9}MIm(FH)_{1.8}F$, (e) $C_{8F13}MIm(FH)_{2.0}F$, and (f) $C_{10F17}MIm(FH)_{2.0}F$.
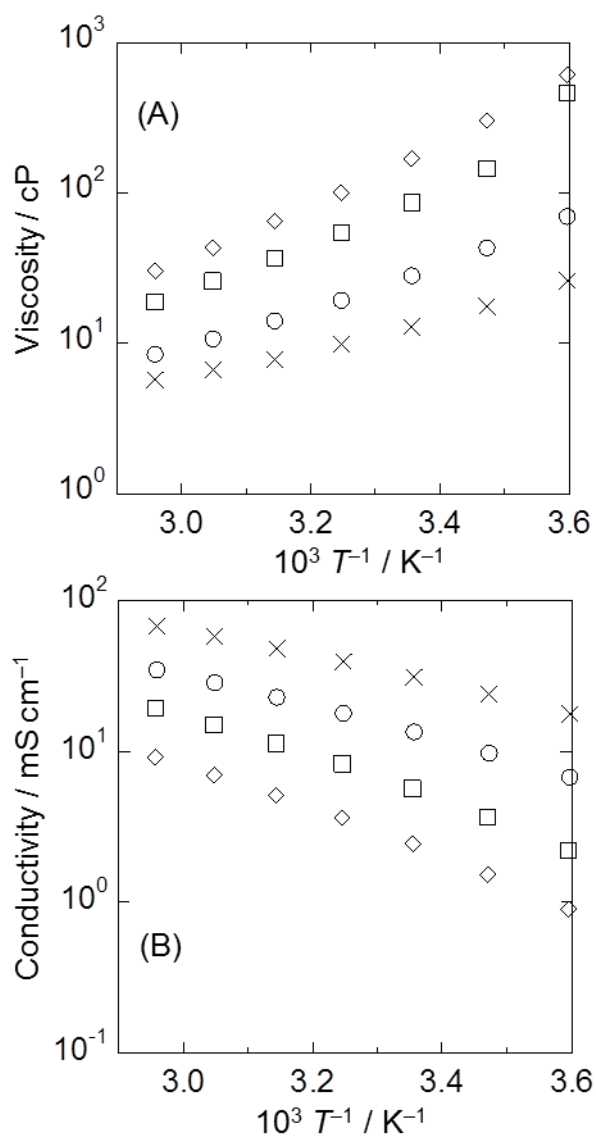
Fig. 4 Arrhenius plots of (A) viscosity and (B) ionic conductivity for $C_3MIm(FH)_{1.7}F$ ($\times$), $C_{3F3}MIm(FH)_{1.7}F$ ($\circ$), $C_{4F5}MIm(FH)_{1.7}F$ ($\square$), and $C_{6F9}MIm(FH)_{1.8}F$ ($\diamondsuit$).
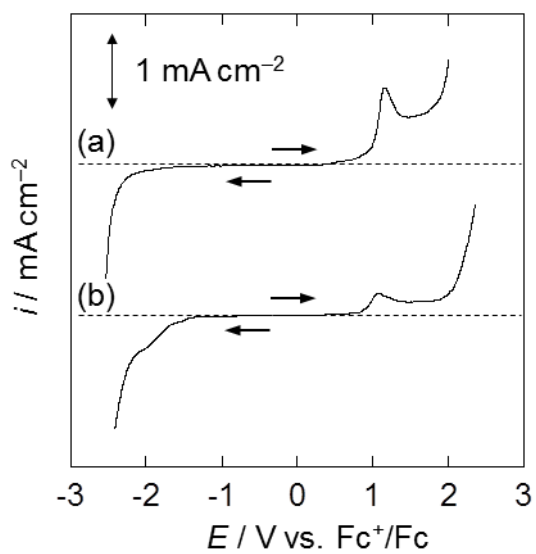
Fig. 5 Linear sweep voltammograms of a vitreous carbon electrode in (a) $C_3MIm(FH)_{1.7}F$, (b) $C_{3F3}MIm(FH)_{1.7}F$. Scan rate: 10 mV s^{-1}.
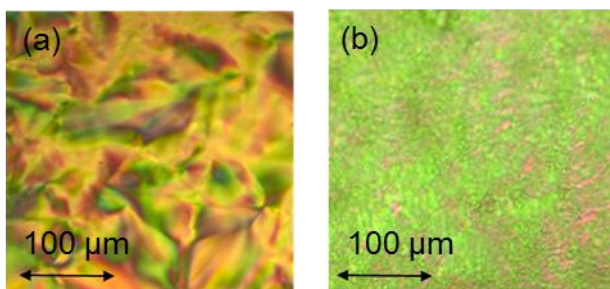
Fig. 6 Polarized optical microscopic textures of (a) $C_{8F13}MIm(FH)_{2.0}F$ at 373 K on cooling from isotropic liquid phase and $C_{10F17}MIm(FH)_{2.0}F$ at 373 K on heating from crystal phase.
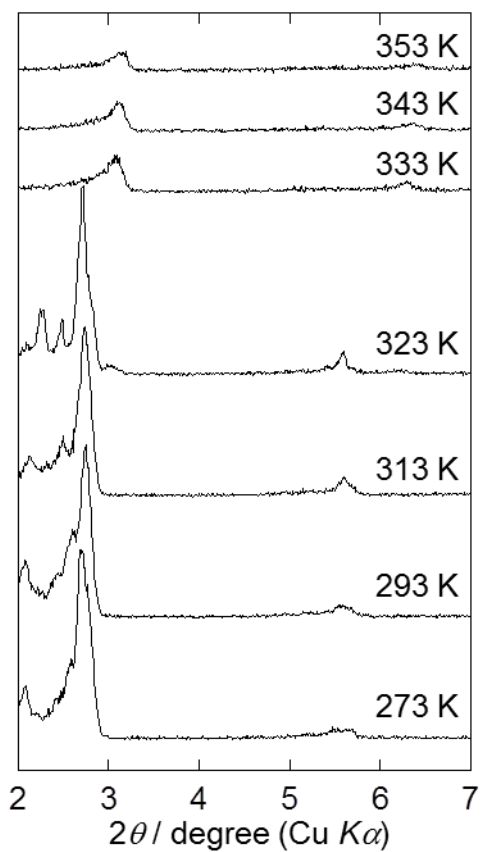
Fig. 7 X-ray diffraction patterns in the low-angle region for $C_{8F13}MIm(FH)_{2.0}F$ in the crystal phase (273–323 K) and the liquid crystal phase (333–353 K).
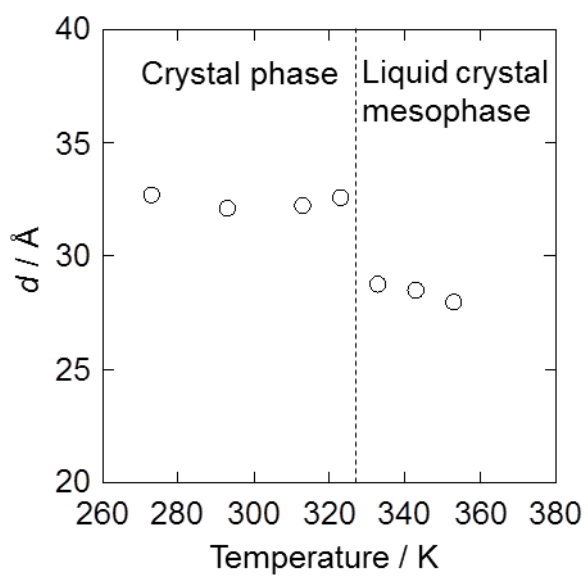
Fig. 8 Layer spacing of $C_{8F13}MIm(FH)_{2.0}F$ in the crystal phase and liquid crystal phase at different temperatures.
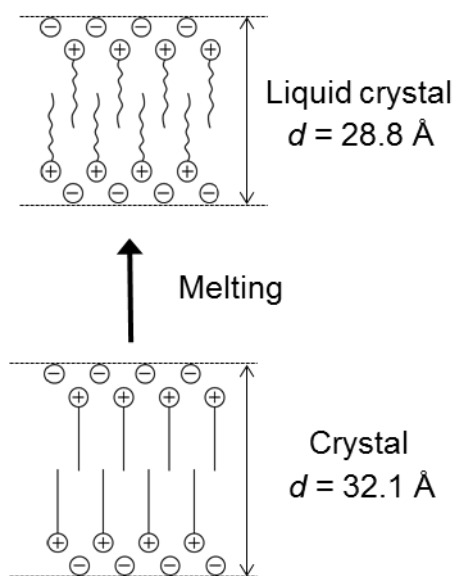
Fig. 9 Schematic illustration of the crystal–liquid crystal phase transition of $C_{8F13}MIm(FH)_{2.0}F$.

References

[1]   J. S. Wilkes, Green Chem. 4 (2002) 73–80.

[2]   K. R. Seddon, J. Chem. Tech. Bioethnol. 68 (1997) 351–356.

[3]   R. Hagiwara, Y. Ito, J. Fluorine Chem. 105 (2000) 221–227.

[4]   H. Xue, R. Verma, J. M. Shreeve, J. Fluorine Chem. 127 (2006) 159–176.

[5]   J. S. Wilkes, M. J. Zaworotko, J. Chem. Soc., Chem. Commun. 13 (1992) 965–967.

[6]   T. Tsuda, C. L. Hussey, Electrochem. Soc. Interface Spring (2007) 42–49.

[7]   A. B. McEwen, H. L. Ngo, K. LeCompte, J. L. Goldman, J. Electrochem. Soc. 146 (1999) 1687–1695.

[8]   M. Armand, F. Endres, D. R. MacFarlane, H. Ohno, B. Scrosati, Nat. Mater. 8 (2009) 621–629.

[9]   T. Welton, Chem. Rev. 99 (1999) 2071–2083.

[10]   S. G. Cull, J. D. Holbrey, V. Vargas-Mora, K. R. Seddon, G. J. Lye, Biotechnol. Bioeng. 69 (2000) 227–233.

[11]   R. Hagiwara, T. Hirashige, T. Tsuda, Y. Ito, J. Fluorine Chem. 99 (1999) 1–3.

[12]   R. Hagiwara, T. Hirashige, T. Tsuda, Y. Ito, J. Electrochem. Soc. 149 (2002) D1–D6.

[13]   M. Yamagata, S. Konno, K. Matsumoto, R. Hagiwara, Electrochem. Solid-State Lett. 12 (2009) F9–F12.

[14]   K. Matsumoto, R. Hagiwara, Y. Ito, Electrochem. Solid-State Lett. 7 (2004) E41–E44.

[15]   S. Kanematsu, K. Matsumoto, R. Hagiwara, Electrochem. Commun. 11 (2009) 1312–1315.

[16]   R. Taniki, K. Matsumoto, R. Hagiwara, Electrochem. Solid-State Lett. 15 (2012) F13–F15.

[17]   Y. Saito, K. Hirai, K. Matsumoto, R. Hagiwara, Y. Minamizaki, J. Phys. Chem. B 109 (2005) 2942–2948.

[18]   T. Enomono, Y. Nakamori, K. Matsumono, R. Hagiwara, J. Phys. Chem. C 115 (2011) 4324–4332.

[19] A. Senda, K. Matsumoto, T. Nohira, R. Hagiwara, J. Power Sources 195 (2010) 4414–4417.

[20] R. Hagiwara, T. Nohira, K. Matsumoto, Y. Tamba, Electrochem. Solid-State Lett. 8 (2005) A231–A233.

[21] H. Matsumoto, T. Matsuda, T. Tsuda, R. Hagiwara, Y. Ito, Y. Miyazaki, Chem. Lett. (2001) 26–27.

[22] V. R. Koch, C. Nanjundiah, R. T. Carlin, U. S. Patent (1998) 5,827,602.

[23] R. P. Singh, S. Manandhar, J. M. Shreeve, Tetrahedron Lett. 43 (2002) 9497–9499.

[24] H. Xue, J. M. Shreeve, Eur. J. Inorg. Chem. 13 (2005) 2573–2580.

[25] T. L. Merrigan, E. D. Bates, S. C. Dorman, J. H. Davis, Jr., Chem. Commun. 20 (2000) 2051–2052.

[26] B. R. Caes, J. B. Binder, J. J. Blank, R. T. Raines, Green Chem. 13 (2011) 2719–2722.

[27] J. J. Tindale, P. J. Ragogna, Chem. Commum. 14 (2009) 1831–1833.

[28] R. Hagiwara, K. Matsumoto, Y. Nakamori, T. Tsuda, Y. Ito, H. Matsumoto, K. Momota, J. Electrochem. Soc. 150 (2003) D195–D199.

[29] F. Xu, K. Matsumoto, R. Hagiwara, Chem. Eur. J. 16 (2010) 12970–12976.

[30] B. K. M. Chan, N.-H. Chang, M. R. Grimmett, Aust. J. Chem. 30 (1977) 2005–2013.

[31] M. E. Wieser, T. B. Coplen, Pure Appl. Chem. 83 (2011) 359–396.

[32] A. Bondi, J. Phys. Chem. 68 (1964) 441–451.

[33] R. D. Shannon, Acta. Cryst. A32 (1976) 751–767.

[34] G. D. Smith, O. Borodin, J. J. Magda, R. H. Boyd, Y. Wang, J. E. Bara, S. Miller, D. L. Gin, R. D. Noble, Phys. Chem. Chem. Phys. 12 (2010) 7064–7076.

[35] K. Binnemans, Chem. Rev. 105 (2005) 4148–4204.

[36] A. E. Bradley, C. Hardacre, J. D. Holbrey, S. Johnston, S. E. J. McMath, M. Nieuwenhuyzen, Chem. Mater. 14 (2002) 629–635.

[37] Z. Wei, X. Wei, S. Fu, J. Liu, D. Zhang, Acta Cryst. E65 (2009) o1159-o1159.

[38] F. Xu, K. Matsumoto, R. Hagiwara, Dalton Trans. 42 (2013) 1965-1968.